

Blends of Etheric Polyitaconates and Polyacrylates with Acidic Polymers

Christine J. T. Landry,* Bradley K. Coltrain, and David M. Teegarden

Corporate Research Laboratories, Eastman Kodak Company,
Rochester, New York 14650-2116

Wayne T. Ferrar

Office Imaging, Eastman Kodak Company, Rochester, New York 14650-2129

Received February 2, 1993; Revised Manuscript Received June 25, 1993*

ABSTRACT: The miscibility between polyitaconates and polyacrylates containing etheric side chains and polymers bearing an acidic functionality, such as poly(vinylphenol) (PVPh) and its copolymers with styrene, and poly(styrene-co-styrene-4-sulfonic acid), is investigated. Heats of mixing measurements are performed on model compounds of these polymers, revealing that the interactions are dominated by the etheric side chains, even though the polyitaconates also contain carbonyl groups that are good hydrogen bond acceptors. These results are confirmed by infrared spectroscopy studies on the blends of both the model compounds and the polymers. Although hydrogen bonding to the carbonyl is evident in blends of poly(methyl methacrylate) with PVPh, little or no hydrogen bonding to the carbonyl of the etheric polyitaconate was observed. The compositional dependences of the glass transition temperature, as obtained by differential scanning calorimetry, exhibit a positive deviation from additivity for blends of PVPh with polymers with low ethylene oxide content and a negative deviation from additivity when the ethylene oxide content is increased.

Introduction

Miscibility in polymers can be enhanced by tailoring polymers with functional groups that are capable of interacting with each other. Interactions such as hydrogen bonding, dipolar coupling, and ion-ion or ion-dipole pairing have been utilized in the past to enhance miscibility in otherwise immiscible polymers. Owing to the fact that high molecular weight polymers have large molar volumes, the combinatorial entropy contributions (which are the primary driving forces for miscibility in small molecule-small molecule or polymer-small molecule mixtures) to the free energy of mixing will be small. Therefore, enthalpic contributions usually dominate in polymeric systems. Polymer miscibility is enhanced as a direct result of a negative enthalpy of mixing (ΔH_m) contribution to the overall free energy of mixing (ΔG_m). When only dispersive or van der Waals forces are present, the enthalpy of mixing depends on the square of the difference in the solubility parameters of the two polymers, which will always be positive or zero. However, a negative ΔH_m can result from specific interactions between the two polymers. The enthalpy of mixing can then be written in the empirical form

$$\Delta H_m/V = RT(\chi_{ij}/v^\circ)\phi_i\phi_j \quad (1)$$

where χ_{ij} is the binary interaction parameter, ϕ is the volume fraction, V is the total volume, and v° is an arbitrary segment volume, not easily defined for polymers. It is often preferable to define a normalized quantity to represent the interaction parameter.

$$\tilde{\chi}_{ij} = \chi_{ij}/v^\circ \quad (2)$$

Calorimetry is used herein to gain insight about ΔH_m , which is fundamental to the understanding of polymer-polymer miscibility. The approach adopted here, as has been used in the past,¹⁻³ is to measure the heats of mixing of low molecular weight models of the polymers. Although the choice of model structures remains subjective and

different models can give somewhat different results, valuable insight and quantitative information can be obtained from these measurements. Typically, the model compounds are chosen to have structures that are similar to the monomeric unit of the polymer or are dimeric or cyclic derivatives of this unit. Mixing is done readily when the model compounds are in the melt state. Since ΔH_m results from changes in energy associated with nearest-neighbor contacts, it should be independent of molecular weight, to a first approximation, unless strong steric restrictions associated with the polymer are present. An interaction parameter, χ_{ij} , between the two compounds can be obtained via these experiments (eqs 1 and 2). Since the blending of highly interacting polymers, such as those reported here, involves breaking and re-forming highly directional hydrogen bonds and, thus, changes in overall degrees of freedom, noncombinatorial entropic contributions are also important in determining their miscibility. These considerations have been addressed extensively by others.^{4,5}

In a previous study,³ the miscibility of polyphosphazenes with polymers containing acidic functional groups was shown to be enhanced (via hydrogen bonding) when the side groups on the polyphosphazene were ethylene oxide. Thus, poly[bis[(methoxyethoxy)ethoxy]phosphazene] (MEEP) and poly[bis[[[(methoxyethoxy)ethoxy]ethoxy]phosphazene] (MEEEP) were shown to be miscible with poly(vinylphenol) (PVPh) over the entire composition range. Additionally, PVPh is known to be miscible with poly(ethylene oxide) (PEO)⁶ and with poly(methyl methacrylate) (PMMA) (see ref 2 and references therein).

Etheric polyitaconates are prepared from the esterification of itaconic acid and contain ethylene oxide side chains. These polymers can be considered as carbon backbone analogs of the etheric polyphosphazene, MEEP. The properties of a variety of polyitaconates have been investigated by Cowie.⁷ Miscibility in copolymer blends of poly(styrene-co-acrylonitrile) with poly(phenyl itaconate-co-methyl methacrylate) has been observed.⁸ The miscibility in these systems is thought to arise not from any effective specific interaction between the components

* Abstract published in *Advance ACS Abstracts*, September 1, 1993.

Table I. Model Compounds

abbrev	mol wt	structure	melt dens (g/mL)
EPH	122.2		0.988
MIB	102.2		0.856
ME-1	190.3		0.959
ME-2	336.4		1.074
EEE	162.3		0.909
TDME	222.3		1.009
(MEEP) ₃	849.8		1.175

of the blend, but primarily from unfavorable interactions between the monomer pairs within an individual copolymer. Poly(monobenzyl itaconate) (PMBI) has been shown to be miscible with poly(*N*-vinylpyrrolidone) (PVP)⁹ and with poly(ethylene oxide)¹⁰ (PEO) but not with poly(vinylidene fluoride).¹¹ The driving force for miscibility in these systems is presumably a result of specific interactions (hydrogen bonding) between the carboxylic acid group on the PMBI and the carbonyl or the ether groups on PVP or PEO, respectively.

In the present study, the miscibility of etheric polyitaconates and etheric polyacrylates with PVPh, poly(styrene-*co*-vinylphenol) [P(S-VPh)] and poly(styrene-*co*-styrenesulfonic acid) [P(S-SA)] is investigated (see Tables I and II). Also, the origins and relative strengths of the interactions governing miscibility of these polymers are investigated as the molecular structure of the hydrogen bond acceptor is varied from PEO to PMMA to the etheric itaconates (which could be viewed as a combination of PEO and PMMA), to the etheric polyphosphazenes (where the backbone is now very different). Calorimetry and infrared spectroscopy provide information about the interactions between model compounds of the various species. Blends of the polymers are characterized by differential scanning calorimetry (DSC) and infrared spectroscopy.

Experimental Section

Materials. 2-(2-Methoxyethoxy)ethanol (Eastman Kodak Co.), triethyleneglycol monomethyl ether (Fluka), and triethylene glycol monoethyl ether (Fluka) were reagent grade and were distilled prior to use. Reagent grade itaconic acid, toluene, and *p*-toluenesulfonic acid 1-hydrate were obtained from Kodak and were used as received. Azobis(2-methylpropanitrile) (AIBN) (Kodak) was recrystallized from methanol. The inhibitor 3-*tert*-butyl-4-hydroxy-5-methylphenyl sulfide (Aldrich) was used as

received. HPLC-grade dimethylformamide (DMF) (OmniSolve, EM Laboratories) was used without further purification. Lithium nitrate was obtained from Aldrich.

Model Compounds. The molecular structures, molecular weights, and densities of the model compounds are listed in Table I. Ethylphenol (EPH) was obtained from Eastman Kodak Co. Methyl isobutyrate (MIB), 2-ethoxydiethyl ether (EEE), and tetraethylene glycol dimethyl ether (TDME) were obtained from Aldrich. The synthesis for the cyclic phosphazene model compound (MEEP)₃ is described elsewhere.³

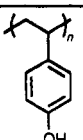
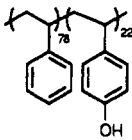
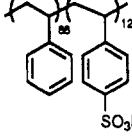
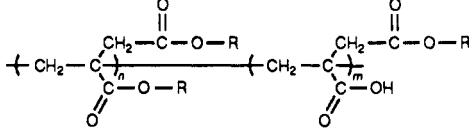
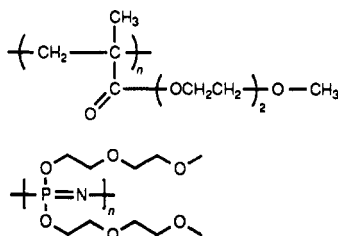
(a) Synthesis of Bis[2-(2-methoxyethoxy)ethyl] Methylsuccinate (ME-2). Into a 500-mL round-bottom flask equipped with reflux condenser, magnetic stirbar, and Dean-Stark receiver were placed 50 g (0.38 mol) of methylsuccinic acid, 93 mL (0.78 mol) of 2-(2-methoxyethoxy)ethanol, 100 mL of toluene, and 1.0 g (5.3 mmol) of *p*-toluenesulfonic acid. The flask was placed in an oil bath at 150 °C and refluxed under an argon flow for 24 h as 13.7 mL of water was collected by azeotropic distillation. The toluene was removed by rotary evaporation, and the product was distilled at 175–178 °C at 0.7 mmHg. ¹H NMR verified the correct product; however, titration of the product indicated 1.97 mol % of unreacted acid groups. The distilled sample was then eluted down a basic alumina chromatographic column (2 in. × 12 in.) using methylene chloride as the eluant. The product was vacuum distilled as before, yielding a colorless liquid having 0.035 mol % of the acid impurity.

(b) Synthesis of [2-(2-Methoxyethoxy)ethyl] Isobutyrate (ME-1). Into a 500-mL round-bottom flask equipped with a reflux condenser, argon inlet, and mechanical stirrer were placed 100 mL of CH₂Cl₂, 47.6 mL (0.40 mol) of 2-(2-methoxyethoxy)ethanol, and 53 mL (0.38 mol) of triethylamine. The flask was cooled in an ice bath as 40 g (0.38 mol) isobutyryl chloride was added dropwise with stirring. After complete addition, the solution was allowed to warm to room temperature. Triethylamine hydrochloride was then removed by filtration, and CH₂Cl₂ was removed by rotary evaporation. The product was vacuum distilled at 73 °C at 0.6 mmHg, yielding 61.1 g (85 %) of colorless liquid. ¹H NMR verified the correct product. Further purification was afforded by eluting the product down a basic alumina chromatographic column (2 in. × 12 in.) using methylene chloride as the eluant and redistilled at 64–65 °C at 0.7 mmHg. Titration results showed <0.008 wt % acid impurity.

Polymers. The structures and available characterization information of the homopolymers and copolymers are presented in Table II. Poly(methyl methacrylate) (PMMA) was purchased from Aldrich and has a molecular weight of $M_w = 93\,000$ and a polydispersity of 2.0, as provided by the manufacturer. Polystyrene (PS) was Styron 666 from Dow Chemical Co. and has a molecular weight $M_w = 241\,000$ with a polydispersity of 3.0. Detailed synthesis and characterization information for poly(vinylphenol) (PVPh), poly(styrene-*co*-vinylphenol) containing 22 mol % VPh [P(S-VPh(22))], and poly(styrene-*co*-styrene-4-sulfonic acid) containing 12 mol % SA [P(S-SA(12))] are reported elsewhere.²

(a) Synthesis of Bis[2-(2-methoxyethoxy)ethyl] Itaconate (MEE-it). This monomer was synthesized by esterification of itaconic acid by a modification of the procedure of Cowie and Ferguson.⁷ Into a 1-L round-bottom flask equipped with reflux condenser, magnetic stirbar, and Dean-Stark receiver were placed 150 g (1.16 mol) of itaconic acid, 292 mL (2.45 mol) of 2-(2-methoxyethoxy)ethanol, 300 mL of toluene, and 2.0 g (10.5 mmol) of *p*-toluenesulfonic acid. The flask was placed in an oil bath at 150 °C and refluxed under an argon flow for 24 h as 41.3 mL of water was collected by azeotropic distillation. The resulting solution was split into two equal portions and treated as follows, designated as procedures A and B for convenience. The toluene in sample A was removed on a rotary evaporator, and the inhibitor 3-*tert*-butyl-4-hydroxy-5-methylphenyl sulfide was added. The sample was then distilled, collecting the fraction at ~180 °C at 0.15 mmHg. Sample B was eluted through a basic alumina chromatographic column (2 in. × 12 in.) using dichloromethane as the eluant. The solvent was removed on a rotary evaporator, the inhibitor was added, and the product was distilled as described for sample A. Sample A was found to contain some monomers with unreacted acid groups, whereas these acid impurities are removed by procedure B. Typically, polymers resulting from

Table II. Polymers

abbrev	structure	characterization ^a
PVPh		$\bar{M}_w = 35\text{K (absolute)}$ $\bar{M}_w/\bar{M}_n = 1.7$
P(S-VPh(22))		$\bar{M}_w = 95.6\text{K}$ $\bar{M}_w/\bar{M}_n = 2.0$
P(S-SA(12))		$\bar{M}_w = 241\text{K}$ $\bar{M}_w/\bar{M}_n = 3.0$
P(MEE-it)-(A)		$\bar{M}_w = 117\text{K (absolute)}$ $\bar{M}_w/\bar{M}_n = 1.5$
P(MEE-it)-(B)	$R = -(\text{CH}_2\text{CH}_2\text{O})_x-\text{CH}_3$ $x = 2 \quad n = 0.7 \quad m = 0.3$	
P(MEEE-it)	$R = -(\text{CH}_2\text{CH}_2\text{O})_x-\text{CH}_3$ $x = 2 \quad n = 1.0 \quad m = 0$	
P(MEE-meth)	$R = -(\text{CH}_2\text{CH}_2\text{O})_x-\text{CH}_3$ $x = 3 \quad n = 1.0 \quad m = 0$	
MEEP		$\bar{M}_w = 3 \times 10^6 \text{(absolute)}$

^a Polystyrene equivalent molecular weights unless noted otherwise.

procedure A contain 10–30 mol % acid impurity, whereas those from procedure B contain less than 0.6 mol %.

(b) Synthesis of Bis[2-[2-(2-methoxyethoxy)ethoxy]ethyl] Itaconate (MEEE-it). The esterification reaction was effected as described above for MEE-it using 30.37 g (0.233 mol) of itaconic acid, 81 g (0.49 mol) of triethylene glycol monomethyl ether, 100 mL of toluene, and 1.04 g (5.5 mmol) of *p*-toluenesulfonic acid. This monomer was treated as described above for MEE-it (procedure B) but cannot be distilled. It was collected by removing the solvent on a rotary evaporator.

Polymerization of Itaconate Monomers. The monomers were polymerized in bulk in a similar manner. A 250-mL, three-necked round-bottom flask fitted with a condenser, mechanical stirrer, and an argon inlet was charged with the itaconate monomer. AIBN was added in a ratio of moles of catalyst to moles of itaconate monomer of 0.013. The flask was heated at 60 °C for 17 h under argon flow. The resulting viscous polymer was then dissolved in THF to approximately 20 wt % solids and precipitated into diethyl ether chilled in a dry ice/acetone bath, yielding a colorless, tacky solid. Alternatively, the polymer can be isolated by dissolving in water to 10 wt % solids and dialyzing in a 10K molecular weight cutoff dialysis bag (Union Carbide) for 1–2 days, followed by freeze drying. Thus, polymerization of MEE-it resulted in poly[bis[2-(2-methoxyethoxy)ethyl] itaconate] [P(MEE-it)]. Polymers obtained from the polymerization of portion A of the monomer are denoted P(MEE-it)-(A), and those obtained from portion B are denoted P(MEE-it)-(B). The latter contain essentially no unreacted acid groups. The polymerization of MEEE-it resulted in poly[bis[2-[2-(2-methoxyethoxy)ethoxy]ethyl] itaconate] [P(MEEE-it)]. Molecular weight determination was performed by size exclusion chroma-

tography. Any residual acid groups on the polyitaconate were reacted with a diazomethylating agent (*N*-methyl-*N*-nitroso-*p*-toluenesulfonamide in potassium hydroxide) to produce the methyl ether derivative and prevent adsorption of the polymer to the chromatographic column. The derivatized polymer was dissolved in a 0.01 N LiNO₃ in DMF eluant solution. The absolute molecular weights were then obtained using viscometry detection and a universal viscosity calibration curve. They are typically on the order of $\bar{M}_w = 100\,000$ – $120\,000$, with a polydispersity of ca. 1.5, regardless of the acid composition of the polymer or the length of the alkyleneoxy side group. A more detailed account of the synthesis and characterization of these etheric itaconate monomers and polymers can be found in ref 12.

(c) Synthesis of [2-(2-Methoxyethoxy)ethyl] Methacrylate (MEE-meth). Into a 500-mL round-bottom flask equipped with a reflux condenser, argon inlet, and mechanical stirrer were placed 50 mL (0.518 mol) of methacryloyl chloride (Aldrich) and 30 mL of methylene chloride. The flask was placed in an ice bath. To this solution was added dropwise with stirring at 10 °C a solution of 100 mL of methylene chloride, 62.5 mL (0.525 mol) of 2-(2-methoxyethoxy)ethanol, and 72.2 mL (0.518 mol) of triethylamine. After 2 h the solution was filtered to remove triethylamine hydrochloride and was concentrated on a rotary evaporator. The product was then eluted down a basic alumina chromatographic column (2 in. × 12 in.) using methylene chloride as the eluant. The solvent was removed on a rotary evaporator and the product distilled, collecting the fraction distilling at 62–64 °C at ≈0.2 mmHg. Polymerization to poly[[2-(2-methoxyethoxy)ethyl] methacrylate] [P(MEE-meth)] was performed by dissolving 25 g of the monomer in 141 mL of THF. The solution was degassed and placed under Ar and 0.5% (0.11 g) AIBN was

Table III. Blend Results

blend	solvent	film	DSC results ^a
P(MEE-it)-(B)/PS	MEK	opaque	2
P(MEE-it)-(B)/PMMA	MEK	opaque	2
P(MEE-it)-(A)/PVPh	THF	clear	1
P(MEE-it)-(B)/PVPh	THF	clear	1
P(MEE-it)-(B)/P(S-VPh(22))	MEK	clear	1
P(MEE-it)-(B)/P(S-SA(12))	MEK	clear	1
P(MEEE-it)/PVPh	MEK	clear	1
P(MEE-meth)/PVPh	MEK	clear	1

^a Key: (1) a single T_g at each composition; (2) two T_g values at each composition unshifted from the values of the individual polymers.

added. The flask was heated at 70 °C for 24 h under Ar. Ether was added to the flask that was cooled in dry ice/acetone to precipitate the polymer. The yield was 95%.

Preparation of Blends. The polymer blends were prepared by dissolving each component in a common, good solvent (either MEK or THF) at 5 wt % and combining the solutions in the appropriate amounts. Most of the solutions were cast into shallow dishes, allowing for slow solvent removal to obtain equilibrium morphology. Polymer blend samples for FTIR measurements were spin-coated from solution onto KBr disks. Spectra of the model compounds were obtained on neat mixtures, deposited between KBr disks.

Details concerning the preparation of the individual blends are reported in Table III. The blend samples were dried under vacuum from ambient temperature to a temperature that is close to or above the glass transition temperature (T_g) of the blend. The maximum drying temperature was kept below 170 °C to prevent degradation.

Experimental Techniques. ΔH_m values were obtained using a Setaram C-80 temperature-controlled calorimeter equipped with a reversing mechanism. The compounds are placed in separate chambers arranged as concentric cylinders with the top of each cell open to a small common vapor space. Typically, the total sample volume was 2 mL. The measurements were performed at 50.0 ± 0.1 °C, chosen such that all components are in the melt state and have a low viscosity.

When literature values were not available, the densities of the components were measured in the melt state using calibrated pycnometers.

Differential scanning calorimetry (DSC) was performed on either a Perkin-Elmer DSC-7 or a Du Pont 990 thermal analyzer equipped with a data-analysis program by Laboratory Micro Systems, Inc. The heating rate used was 20 °C/min.

FTIR spectra of the blends and mixtures were obtained using either a Bio-Rad (Digilab Division) FTS-7 spectrometer (3240-SPC) or a Nicolet 60SX FTIR spectrometer at a resolution of 4 cm⁻¹. Infrared spectra of the monomers and polymers were obtained on a Nicolet 5SXB FTIR spectrometer. The percent acid in itaconate monomers and polymers was obtained by titration with hexadecyltrimethylammonium hydroxide using a Metrohm E670 Titroprocessor, a Metrohm E665 Dosimat equipped with a 1-mL buret, and a combination glass electrode.

¹H NMR spectra were obtained on a General Electric Model QE-300 (300-MHz) spectrometer using CDCl₃ as both internal standard and solvent.

Results and Discussion

Model Studies. 4-Ethylphenol (EPH) is used as a model for poly(vinylphenol), a hydrogen bond donor. The model compound chosen to represent the MEE itaconate polymer [P(MEE-it)] is ME-2 (see Table I) where the ether is the primary proton acceptor. Other models are chosen in order to vary the acceptor from acrylate (using a model for PMMA, i.e., MIB) to ether (using a model for PEO, i.e., TDME). The enthalpies of mixing between EPH and these other models were also measured, and the results are plotted in Figure 1 in kcal/mol as a function of mol % EPH. Also plotted in this figure are results (previously reported³) for mixtures of EPH with cyclic etheric phos-

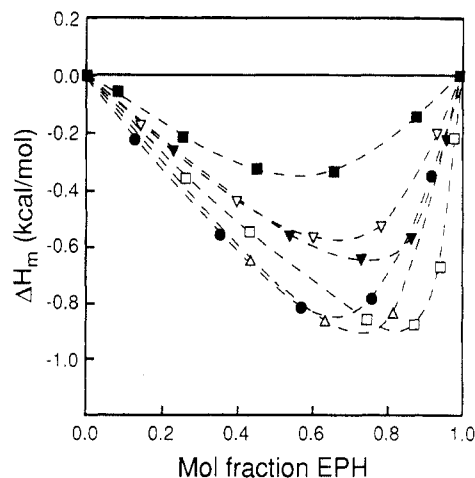


Figure 1. Compositional dependence of the heats of mixing for mixtures of EPH with (■) MIB, (Δ) TDME, (●) EEE, (▽) ME-1, (▼) ME-2, and (□) (MEEP)₃.

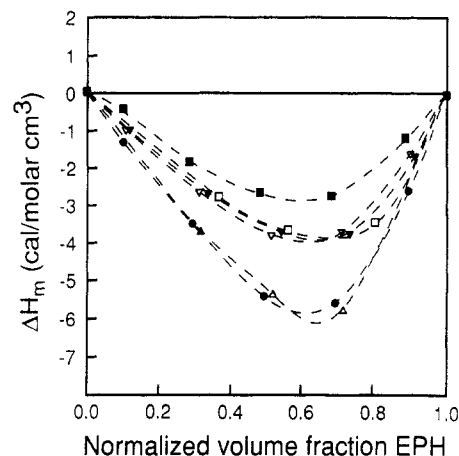


Figure 2. Compositional dependence of the heats of mixing for the same mixtures as in Figure 1, normalized by the molar volume of each component.

phazene (MEEP)₃. As a result of the mismatch in the molecular weights and volumes of the etheric compounds relative to those of EPH and to each other, the curves in Figure 1 do not have similar symmetry with respect to composition. An alternate way of comparing the ΔH_m values of EPH with each of the models is illustrated in Figure 2. The number of moles of each model compound has now been normalized by its molar volume, as calculated from group contribution methods.^{4,13} The normalized enthalpy values are plotted against the normalized volume fractions. The results for mixtures of MIB with EPH (previously reported²) are also shown.

The large, exothermic ΔH_m values obtained indicate strong interactions between the phenol and each of the models. The magnitude of these measured enthalpies is consistent with that expected for hydrogen bonding interactions. The strength of the interaction between EPH and both etheric itaconate models, as well as the etheric phosphazene, falls intermediate between that with the ester (MIB) and that with the ethers (TDME and EEE).

More information about the relative strengths of these interactions was obtained by infrared spectroscopy. Figure 3 shows the hydroxyl (OH) stretching regions of the FTIR spectra for pure EPH, and for 50/50 wt % blends with TDME, EEE, MIB, ME-1, and ME-2. These spectra were obtained at 50 °C and, therefore, should correlate exactly with what was observed in the calorimetric experiments. The broad OH band is often deconvoluted into several overlapping bands, where the higher wavenumber (ca.

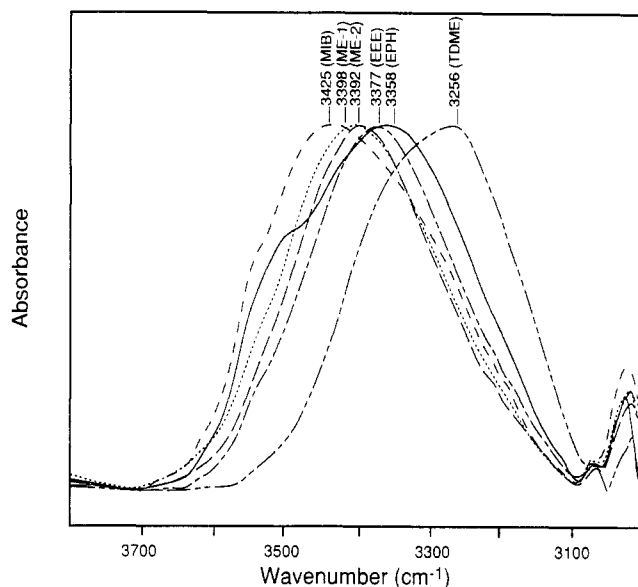


Figure 3. Hydroxyl stretching region of the infrared spectra for pure melts of (—) EPH, and 50/50 wt % mixtures with (— · —) EEE, (— · · —) TDME, (· · ·) MIB, (···) ME-1, and (— · —) ME-2 at 50 °C.

3520–40 cm^{-1}) band is due to unbound or “free” hydroxyls and the lower frequency bands are due to homo- and heterobound hydroxyl groups. As the OH groups become more highly hydrogen-bound, the peak maximum shifts from its original position, with a concomitant decrease in the amount of free OH groups. This reflects a redistribution in the amount of self-associated vs heteroassociated OH groups in the mixtures. The strength of the heteroassociation controls the peak shape and position of the maximum. The peak maximum for 50/50 mixtures of EPH/(MEEP)₃ was previously reported³ to occur at 3358 cm^{-1} . The frequency shift ($\Delta\nu$), reflected by the difference between the free hydroxyl peak absorbance (ca. 3520 cm^{-1}) and that of the bound peak maximum, has been correlated with the enthalpy of hydrogen bond formation for several monomeric systems.¹⁴ The enthalpy of mixing comprises contributions from the enthalpy of hydrogen bond formation and equilibrium constants for the self-associating species and for the heteroassociating species, as well as contributions from dispersive forces. If one assumes that the dispersive contributions are small relative to the interaction terms and holds the self-associating species constant, as in the present comparison, then the enthalpy of mixing can be related to the enthalpy of hydrogen bond formation between components.

Differences in equilibrium constants for ether–phenol and ester–phenol associations will also affect the comparison. The curve, obviously, will not pass through the origin. Figure 4 shows the correlation between the enthalpy of mixing and $\Delta\nu$ obtained for the systems at hand and indicates a surprisingly reasonable agreement between the two experiments. Such correlations have been observed by others.¹⁵ The exceptions to this correlation are the results for EPH/EEE. Whereas the calorimetric results obtained for EPH with EEE are nearly identical to those for EPH with TDME, the infrared shift in the hydroxyl band is markedly smaller in the former. This may reflect a dilution of end groups (or aliphatic character) as the length of the etheric chains is increased. However, a number of ethers were examined and the frequency shifts did not follow this trend absolutely. Also, changing the ends of EEE from ethyl to methyl had no effect, suggesting that we are not observing end group effects. The $\Delta\nu$ obtained for the TDME mixture is nearly identical to that

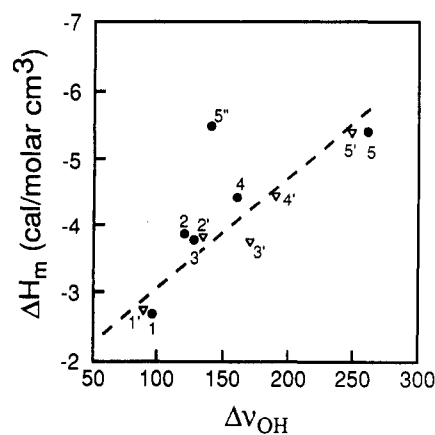


Figure 4. Correlation between ΔH_m (normalized) of model compounds and $\Delta\nu_{\text{OH}}$ for 50/50 wt % mixtures of (●) model compounds and (▼) polymers. The numbers correspond to (1) MIB, (1') PMMA, (2) ME-1, (2') P(MEE-meth), (3) ME-2, (3') P(MEE-it)-(B), (4) (MEEP)₃, (4') MEEP, (5) TDME, (5') PEO, (5'') EEE.

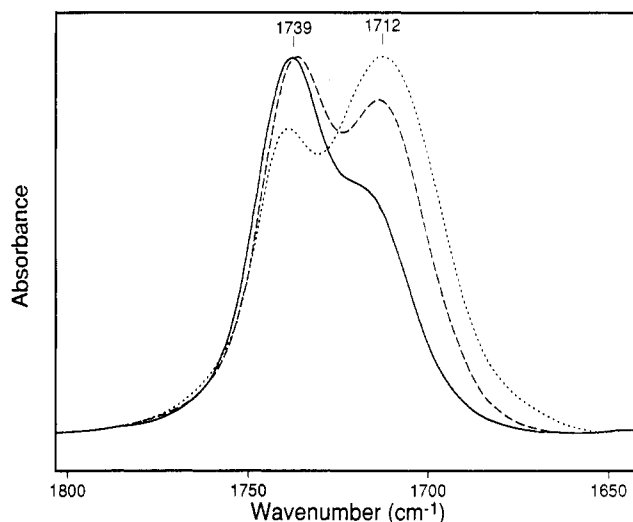


Figure 5. Carbonyl stretching region of the infrared spectra for 50/50 wt % mixtures of (···) EPH/MIB, (— · —) EPH/ME-1, and (—) EPH/ME-2 at 50 °C.

observed for polymer blends of PVPh with PEO.⁶ The model EEE was chosen and is important because it is closer in chain length to the side chains of P(MEE-it) and MEEP. These results may also shed some light into differences in the strength of the interactions between PVPh and MEEP compared to PEO. It is not understood at this time why the infrared results are different for EEE. One may speculate that the chain length (three oxygens) may be optimal for multiple coordination to the phenol (chelating effect). Only the results for 50/50 wt % mixtures are shown here, although 30/70 and 70/30 wt % mixtures were also examined and gave identical results. There was little variation in the frequency of the peak maximum with composition.

The strength of the phenol/ether interaction is greater than that of the phenol/ester interaction. The strengths of the phenol/etheric itaconate interactions fall intermediate between these. Also shown in this figure are the results for the corresponding polymeric blends.

The participation of the ester carbonyl in the hydrogen bonding interactions can also be seen from FTIR. Figure 5 shows the carbonyl stretching region for 50/50 wt % mixtures of EPH with MIB, ME-1, and ME-2. In all cases a new peak appears at lower frequency arising from hydrogen-bound carbonyls. The carbonyl band can be curvefit into two overlapping peaks, one representing free

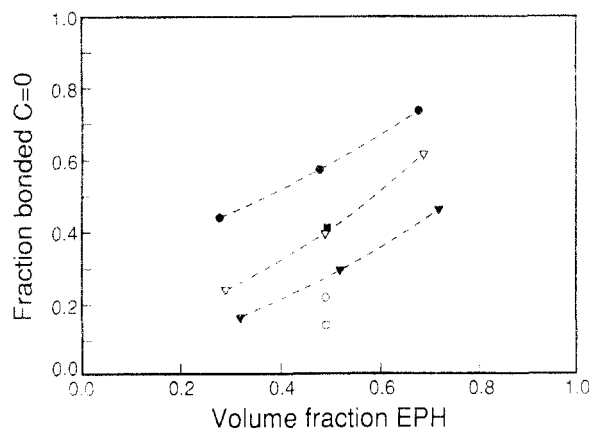


Figure 6. Compositional dependence of the fraction of bound carbonyls in mixtures of (●) EPH/MIB, (▼) EPH/ME-1, and (▼) EPH/ME-2. Also shown are the results for 50/50 wt % blends of (■) PVPh/PMMA, (○) PVPh/P(MEE-meth), and (□) PVPh/P(MEE-it)-(B).

carbonyls and the other (at lower frequency) representing bound carbonyls. The peak areas have been corrected for differences in absorptivities of the free and bound carbonyl vibrations, using (a_{hb}/a_f) equal to 1.5 (see ref 2 and references therein). A much greater fraction of the carbonyls participates in hydrogen bonding (hb) in the ester [MIB/EPH (57% hb)] mixtures than in the itaconate models [ME-1/EPH (39% hb) and ME-2/EPH (16% hb)] mixtures. Figure 6 shows this to be true at all compositions. This a result of competitive equilibria between the ester/phenol and ether/phenol associations within the same molecule. It has recently been shown by Coleman et al.,¹⁶ for ternary blends of PVPh, PEO, and poly(vinyl acetate), that the equilibrium constant for interassociation is about 4 times larger for the ether blend than for the ester blend. Interestingly, the relative amount of hydrogen-bound carbonyls found in these mixtures of low molecular weight models is much higher than that found experimentally, or predicted,⁴ for similar polymer blends. [Compare the MIB/EPH results to poly(methacrylate)/PVPh blends.⁴]

Polymer Blends with PVPh: Thermal Studies. An overview of the polymer blends and their miscibility with PVPh is reported in Tables III and IV. P(MEE-it) was found to be immiscible with PS and with PMMA. These blends were opaque and exhibited two glass transition temperatures at each composition, unshifted from the T_g values of the pure components. However, when an acidic group is attached to the styrene ring, such as in PVPh, P(S-VPh(22)), and P(S-SA(12)), miscibility is observed. All of the miscible blend films were transparent and exhibited single T_g values. The compositional dependence of the measured T_g , taken as the onset in the change in heat capacity with temperature in the DSC trace, for each blend with PVPh, is shown in Figure 7. Most of these curves could be fit successfully to the Kwei equation¹⁷

$$T_g = (w_1 T_{g1} + k w_2 T_{g2}) / (w_1 + k w_2) + q w_1 w_2 \quad (3)$$

where w_i is the weight fraction of component i . This relation has been successful in fitting the composition dependence of T_g for many miscible blends of strongly interacting polymers. Recently, a more rigorous expression for the compositional dependence of T_g for blends of highly interacting polymers has been published.⁵ Although this has the same general form as the Kwei equation, the fitting parameter q becomes a combination of a composition-dependent term that depends on the balance of self-associating and heteroassociating interactions and a term that reflects the temperature dependence of the specific

Table IV. Glass Transition Temperatures of the Blends

blend	composition	solvent	T_g (°C)	
			onset	midpoint
PMMA/PVPh	100/0	MEK	101	110
	75/25		123	131
	50/50		146	154
	25/75		164	170
	0/100		183	188
P(MEE-it)-(B)/PVPh	100/0	THF	-72	-58
	75/25		11	23
	50/50		66	75
	25/75		115	130
	0/100		-71	-45
P(MEE-it)-(A)/PVPh	100/0	THF	23	36
	75/25		92	104
	50/50		143	156
	25/75		164	170
	0/100		-71	-45
P(MEEE-it)/PVPh	100/0	MEK	-70	-51
	75/25		-8	4
	50/50		47	60
	25/75		113	128
	0/100		-44	-30
P(MEE-meth)/PVPh	100/0	MEK	16	38
	75/25		87	95
	50/50		136	143
	25/75		164	170
	0/100		-72	-58
P(MEE-it)-(B)/P(S-VPh(22))	100/0	MEK	-1	8
	75/25		37	50
	50/50		80	87
	25/75		122	127
	0/100		-72	-58
P(MEE-it)-(B)/P(S-SA(12))	100/0	MEK	15	39
	75/25		87	94
	50/50		108	114
	25/75		116	121
	0/100		116	121

heat of the self-associating components. Unfortunately, the calculation of these terms requires the knowledge of the enthalpies of hydrogen bond formation for the polymers in question. These are not presently known for the blends of this study and therefore the more simple Kwei equation is used.

In consideration of the fact that only a few compositions were studied for each blend series, it was deemed appropriate to fix the parameter k to unity, thus retaining a single adjustable parameter, q . The calculated values for q , listed in the figure caption, characterize the shape of the curve and should theoretically provide a first level indication of the excess stabilization energy present in the blends due to molecular interactions. This reflects a balance of the destabilization of the self-associating polymer and a restabilization as it recombines in the blend. Thus, a large positive value for q supports strong inter-polymer interactions or an overall energetic stabilization. Also shown are the T_g data previously reported² for miscible PMMA/PVPh blends. The P(MEE-meth)/PVPh blends behave similarly to the PMMA/PVPh blends in that both exhibit a positive deviation from additivity and thus positive values for q . The value obtained for the P(MEE-meth)/PVPh blend is higher than that for the PMMA/PVPh blend, suggesting the presence of stronger heterointeractions in the former. However, as the ethoxy content of the itaconate is increased from a monosubstituted [P(MEE-meth)] to a disubstituted [P(MEE-it)-(B)] polymer, and then the side chains are lengthened [P(MEEE-it)], the curves begin to exhibit a negative deviation from additivity. The q value obtained for the P(MEEE-it)/PVPh blends is, in fact, negative. The value obtained for the P(MEE-it)-(B)/PVPh blends is intermediate between that for the P(MEEE-it) and P(MEE-meth) blends and is slightly positive. However, the theoretical curve does not fit the data very well. The results obtained for the blends of PVPh with the acid-containing polyitaconate P(MEE-it)-(A) show a strong positive de-

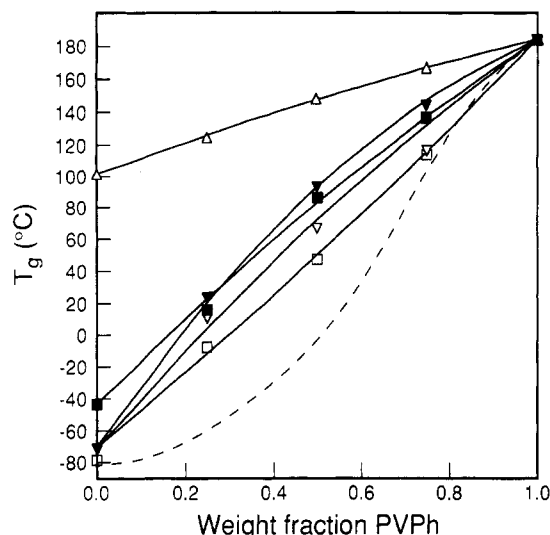


Figure 7. Compositional dependence of the T_g onset for blends of PVPh with (Δ) PMMA ($q = 21$), (\blacksquare) P(MEE-meth) ($q = 51$), (∇) P(MEE-it)-(A) ($q = 144$), (\diamond) P(MEE-it)-(B) ($q = 41$), and (\square) P(MEEE-it) ($q = -29$). The solid lines are theoretical fits to the Kwei equation. The dashed line represents the experimental data for the MEEP/PVPh and MEEP/PVPh blend (data points not shown for clarity).

viation from additivity, in contrast to the blends with the acid-free P(MEE-it)-(B). The reasons for this are unclear at the present but probably reflect differences in the local environment of the individual chains. The presence of ca. 30 mol % acidic substitution (as is the case for the present polymer) can lead to self-association of P(MEE-it) chains, in addition to heteroassociation, thus changing its molecular conformation in the pure state as well as in the blend.

Also shown by the dashed curve in Figure 7 are previously published³ results for MEEP/PVPh blends. The Kwei equation did not reproduce the observed sigmoidal shape of the T_g -composition curve whereas a third power equation (with respect to the concentration of the more rigid polymer) proposed by Brekner, Schneider, and Cantow¹⁸ was successful. This relation considers the effects of binary contact interactions and their influence on conformational redistributions of the chains, and the free volume distribution in the blend. T_g -composition curves with similar sigmoidal shapes have been reported for miscible blends of poly(vinyl methyl ether) (PVME) with PS copolymers functionalized with low levels of 2-hydroxyhexafluoro-2-propanol¹⁹ groups where the heterointeractions are strong, as well as for blends of PVME with PS,²⁰ where these interactions are much weaker. Miscible blends of PVPh and PEO were also observed to exhibit this sigmoidal T_g -composition behavior, although the crystallinity of PEO in these blends was not corrected for.²¹ This must be considered, since it will alter the composition of PEO in the amorphous mixed phase, thus affecting the shape of the curve. The T_g -composition curves for the polyitaconate blends can also be fit to the Brekner¹⁶ relation; however, no new insight was obtained by performing this exercise.

The above discussion illustrates that the character of the T_g -composition curves can be very different for various miscible blends where the strengths of the interactions are very similar. This emphasizes the importance of free-volume effects,²² conformational rearrangements, and local energetic perturbations in the neighborhood of the interacting contact points when predicting the T_g behavior of blends.

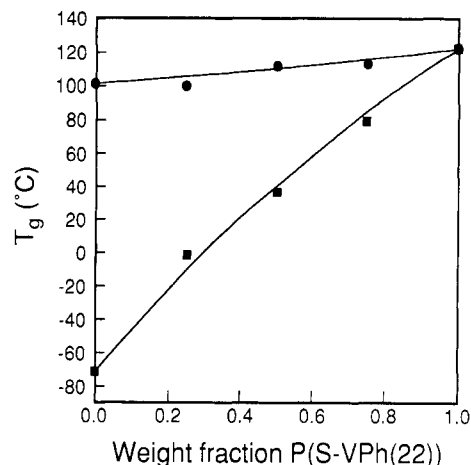


Figure 8. Compositional dependence of the T_g onset for blends of P(S-VPh(22)) with (\bullet) PMMA ($q = -6$) and (\blacksquare) P(MEE-it)-(B) ($q = 64$). The solid lines are theoretical fits to the Kwei equation.

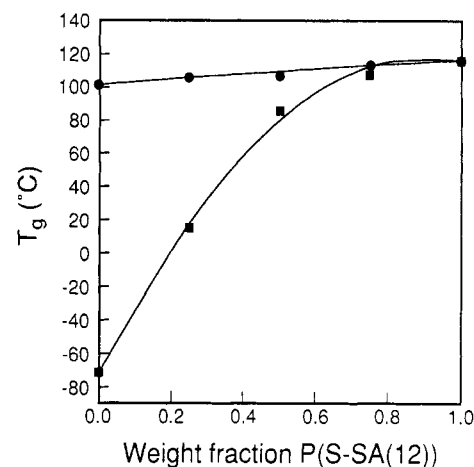


Figure 9. Compositional dependence of the onset T_g for blends of P(S-SA(12)) with (\bullet) PMMA ($q = 3$) and (\blacksquare) P(MEE-it)-(B) ($q = 234$). The solid lines are theoretical fits to the Kwei equation.

Figures 8 and 9 compare the T_g -composition behavior for the miscible blends of P(MEE-it)-(B) or PMMA with P(S-VPh(22)) and P(S-SA(12)), respectively. The solid lines represent fits to the Kwei equation. In both cases, the blends with P(MEE-it) would seem to indicate stronger heterointeractions, particularly with the sulfonic acid-containing blends. Differences in the self-associations present in the sulfonic acid-containing polymers relative to those present in the phenolic polymers will also be reflected in the shape of the T_g -composition curves.

Polymer Blends with PVPh: Infrared Studies. The polymer blends with PVPh were examined by FTIR. All samples were annealed above the T_g of the polymer or the blend prior to obtaining the FTIR spectra. Figure 10 shows the hydroxyl (OH) stretching regions for pure PVPh and for its blends with P(MEE-meth) and with P(MEE-it)-(B). As with the models, the amount of free OH groups (represented by the peak at ca. 3520 cm^{-1}) is seen to decrease in the blends. The frequency shift ($\Delta\nu$) between the free hydroxyl absorbance and that of the bound peak maximum also shifts, as was seen with the mixtures of model compounds. Also marked on the figure are the peak maxima, previously reported, for the 50/50 wt % blends of PMMA/PVPh² and MEEP/PVPh.³ The maximum in the OH peak reported⁶ for a 50/50 blend of PEO/PVPh is ca. 3270 cm^{-1} .

As before, the strength of the phenol/etheric itaconate interactions falls intermediate between that of the phenol/

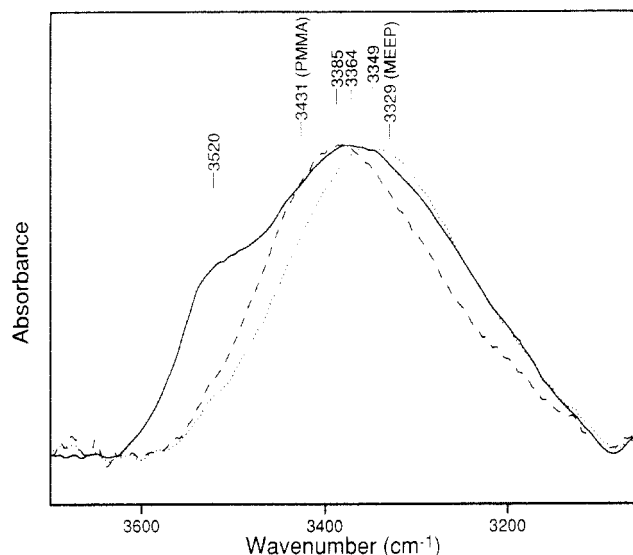


Figure 10. Hydroxyl stretching region of the infrared spectra for pure melts of (—) PVPPh and 50/50 wt % mixtures of PVPPh with (---) P(MEE-meth) and with (...) P(MEE-it)-(B).

ether and of the phenol/ester. As the amount of ether content in the polymer increases, the peak shifts to lower wavenumbers. Although the MEEP phosphazene has only etheric groups, the interaction is weaker than that observed for PEO/PVPPh blends. Whereas this is consistent with the electrophilic nature of the phosphorus atom in the phosphazene backbone,²³ the shift is also in line with that observed for PVME/PVPPh blends (peak maxima occurs at 3320 cm^{-1} for a 50/50 blend⁶) and other ether blends^{24,25} where the etheric group is in a side chain rather than in the backbone. However, blends of PVPPh with poly-(tetramethylene oxide)²⁴ also exhibit a significantly smaller $\Delta\nu$ (ca. 200) than do blends with PEO. The smaller shifts observed for the shorter chain ether models (EEE) are recalled and may reflect a similar phenomenon. The values for $\Delta\nu$ obtained for the polymer blends in this study correlate very well with the heats of mixing results obtained for the model compounds (see Figure 4).

The participation of the ester carbonyl in hydrogen bonding interactions can also be seen from FTIR. Figure 11a shows the carbonyl stretching region for a 50/50 wt % mixture of PVPPh with P(MEE-meth). The results for the curvefit (corrected for absorptivity differences) indicate that only 21% of the carbonyls are involved in hydrogen bonding to the phenol in these blends. This is much lower than what was observed for blends of PMMA/PVPPh (50/50), where the fraction of carbonyls involved in hydrogen bonding to the phenol was closer to 40%.² Evidently, the site for hydrogen bonding preferentially shifts from the carbonyl to the ether groups. The results for a 50/50 wt % blend of P(MEE-it)-(B)/PVPPh are shown in Figure 11b. Now, only ca. 13% of the carbonyls are involved in hydrogen bonding. The carbonyl peak for the P(MEE-it)-(B) itself consists of two overlapping peaks, centered at 1743 and 1728 cm^{-1} , due to the presence of two different types of esters in the molecule. It is difficult to differentiate which carbonyl is most hydrogen-bound, represented by the peak at 1703 cm^{-1} .

Although the repeat unit of the P(MEE-it) polymer has an identical molecular structure to that of the model (ME-2), a much higher fraction of the carbonyls is bound in the latter. This is also the case for the other models compared to the corresponding polymers (see Figure 6). This is probably indicative of less steric constraints in the model system compared to the polymer. In the polymer system,

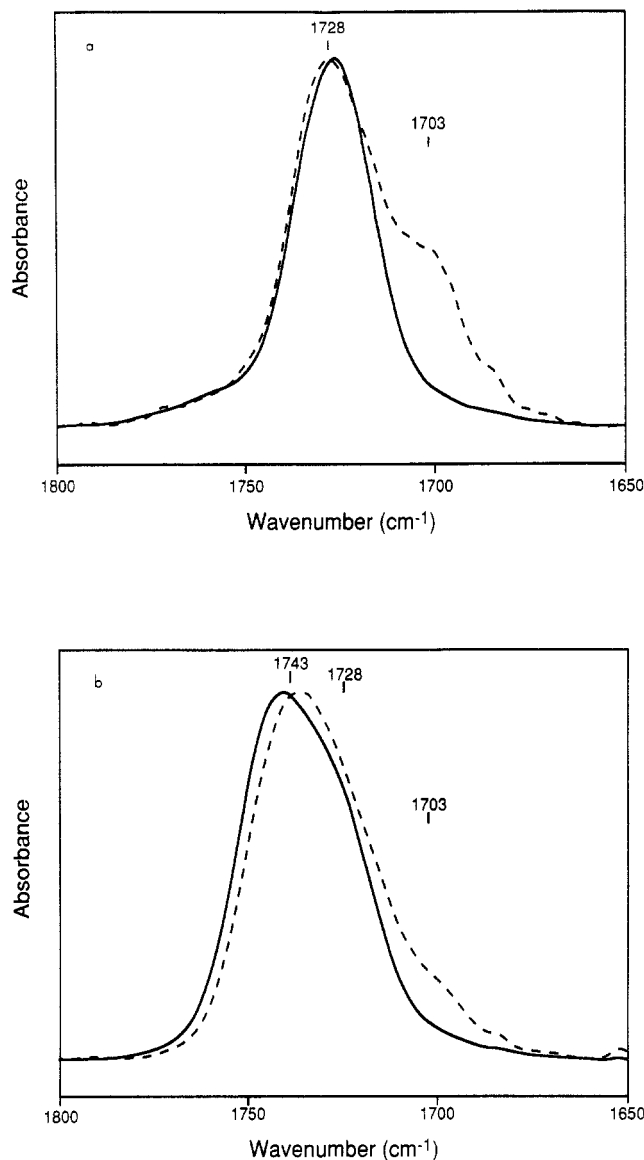


Figure 11. Carbonyl stretching region of the infrared spectra for (a) (—) P(MEE-meth) and (---) a 50/50 wt % blend of PVPPh/P(MEE-meth) and for (b) (—) P(MEE-it)-(B) and (---) a 50/50 wt % blend of PVPPh/P(MEE-it)-(B).

it is likely that the carbonyls are shielded by the ethoxy extensions of the side chains and cannot position themselves in such a way as to be accessible for hydrogen bonding. Thus, two effects are operable. The first, as discussed above, reflects the competitive equilibria between ether/phenol and ester/phenol interaction. The second reflects steric crowding of the carbonyls by the long ethoxy chains combined with constrictions due to backbone flexibility. These effects curtail the participation of the carbonyls in hydrogen bonding to the phenols.

The tendency observed in this work for the polymers to be less prone to hydrogen bonding than the model compounds suggests a correlation with the often observed increased hydrolytic stability of the polymers. The hydrolysis rate of PMMA can be quite different from that of a monomeric model ester. These differences have also been attributed to steric factors, especially the tacticity of the polymer. Syndiotactic or atactic PMMA undergoes hydrolysis in strong acid considerably slower than does isotactic PMMA.²⁶ The first steps in the acid-catalyzed hydrolysis of an ester are protonation of the carbonyl oxygen atom followed by attack at the carbonyl carbon by the nucleophile (water). The shielding of either or both of these ester atoms by neighboring groups could account

for the lowered reactivity of the polymer. Obviously, shielding the carbonyl oxygen would diminish the participation of an ester in hydrogen bonding. A polyitaconate and a polymethacrylate share similar structures. Thus, it is not unreasonable that the carbonyl groups in the polyitaconates discussed above are shielded somewhat sterically from protons and, as a result, participate less in hydrogen bonding than do their small molecule counterparts. Analogously, Allcock has discussed²⁷ the advantages and limitations of using cyclics to model phosphazene polymers. Studies of the small molecules lead to underestimates of the polymer hydrolytic stability.

Conclusions

Blends of several classes of polymers, ranging from acrylates to etheric polyphosphazenes, with acidic organic polymers, were investigated. Etheric polyphosphazenes such as MEEP and MEEP were previously³ found to be miscible with PVPh over the entire composition range. The driving force for this miscibility is thought to be hydrogen bonding between the phenolic moiety and the alkyleneoxy side chains on the MEEP. Etheric polyitaconates, which can be regarded as carbon backbone analogs of the etheric polyphosphazene MEEP, were also found to be miscible with PVPh over the entire composition range. The enthalpy of mixing of low molecular weight models of these polymers indicates the presence of strong interactions between the phenol and the phosphazene, as well as the itaconate, models. The magnitude of the measured ΔH_m for both these systems lies intermediate between those for mixtures of EPH with a simple ester (MIB) and mixtures of EPH with an ether (TDME and EEE).

The observed shapes of T_g -composition curves for the PVPh/MEE(E)P blends are sigmoidal. The blends of the etheric polyitaconates with PVPh did not show this sigmoidal character even though they exhibit interpolymer interactions of comparable strength. Blends of PVPh with P(MEEE-it) come closest to exhibiting this behavior, showing a negative deviation from additivity, whereas blends with P(MEE-it) or P(MEE-meth) behaved more like blends with PMMA and showed a slight positive deviation from additivity.

FTIR reveals that, although the etheric polyitaconates contain carbonyl groups that could potentially participate in hydrogen bonding to the phenol, very few hydrogen-bonded carbonyls are observed in blends of these polymers, relative to blends of PVPh with PMMA. On the other hand, a significant fraction of hydrogen-bonded carbonyls is observed for mixtures of the model compounds of the itaconates with EPH. Local steric effects seem important in determining the participation of the ester carbonyl in hydrogen bonding to the phenol.

Calculations based on a group contribution approach or experimental evidence obtained on small molecule model compounds is frequently used to predict behavior in polymeric systems. In many cases these approximation methods correlate quite well with observations in the polymers, at least qualitatively. At times, however, differences such as those described in the itaconate series

above are observed. It would be desirable, although it is not always possible, to understand these differences so that one could better appreciate the fundamental limitations of the predictive methods. Modeling studies could also offer significant insight.

Acknowledgment. We wish to acknowledge J. M. O'Reilly for valuable discussions, M. R. Landry for computational assistance, and D. E. Margevich for assistance with the infrared analysis. We are also very grateful for the technical assistance of M. Vega and M. Gartley.

References and Notes

- (1) Crux, C. A.; Barlow, J. W.; Paul, D. R. *Macromolecules* **1979**, *12*, 726.
- (2) Landry, C. J. T.; Teegarden, D. M. *Macromolecules* **1991**, *24*, 4310.
- (3) Landry, C. J. T.; Ferrar, W. T.; Teegarden, D. M.; Coltrain, B. K. *Macromolecules* **1993**, *26*, 35.
- (4) Coleman, M. M.; Graf, J. F.; Painter, P. C. *Specific Interactions and the Miscibility of Polymer Blends*; Technomic Publishing Co., Inc.: Lancaster, PA, 1991.
- (5) Painter, P. C.; Graf, J. F.; Coleman, M. M. *Macromolecules* **1991**, *24*, 5630.
- (6) Moskala, E. J. Ph.D. Thesis, 1984.
- (7) (a) Cowie, J. M. G.; Ferguson, R. J. *Polym. Sci., Polym. Phys. Ed.* **1985**, *23*, 2181. (b) Cowie, J. M. G.; Martin, A. C. S. *Polymer* **1991**, *32* (13), 2411.
- (8) Cowie, J. M. G.; Reid, V. M. C.; McEwen, I. J. *Polymer* **1990**, *31*, 486.
- (9) Cesteros, L. C.; Rego, J. M.; Vazquez, J. J.; Katime, I. *Polym. Commun.* **1990**, *31*, 152.
- (10) Quintana, J. R.; Radic, D.; Cesteros, L. C.; Katime, I. A. *Makromol. Chem.* **1986**, *187*, 1457.
- (11) Katime, I. A.; Quintana, J. R.; Cesteros, L. C.; Peleteiro, M. C. *Polym. Bull.* **1989**, *21*, 69.
- (12) Coltrain, B. K.; Ferrar, W. T.; Salva, J. M. *J. Polym. Sci., Polym. Chem. Ed.* **1993**, *31*, 2261.
- (13) Van Krevelen, D. W. *Properties of Polymers*, 3rd ed.; Elsevier Scientific Publishing Co., Inc.: New York, 1990.
- (14) (a) Badger, R. M.; Bauer, S. H. *J. Chem. Phys.* **1937**, *5*, 839. (b) Purcell, K. F.; Drago, R. S. *J. Am. Chem. Soc.* **1967**, *89* (12), 2874.
- (15) Pimentel, G. C.; McClellan, A. L. *The Hydrogen Bond*; W. H. Freeman and Co.: San Francisco, 1960; Chapter 7 (see also references therein).
- (16) Le Menestrel, C.; Bhagwagar, D. E.; Painter, P. C.; Coleman, M. M.; Graf, J. F. *Macromolecules* **1992**, *25*, 7101.
- (17) (a) Kwei, T. K. *J. Polym. Sci., Polym. Lett. Ed.* **1984**, *22*, 307. (b) Lin, A. A.; Kwei, T. K.; Reiser, A. *Macromolecules* **1989**, *22*, 4112.
- (18) (a) Brekner, M.-J.; Schneider, H. A.; Cantow, H.-J. *Polymer* **1988**, *19* (1), 78. (b) Schneider, H. A. *Polymer* **1989**, *30*, 771. (c) Schneider, H. A. *Makromol. Chem.* **1988**, *189*, 1941. (d) Schneider, H. A. *Polymer* **1989**, *30*, 771.
- (19) Pearce, E. M.; Kwei, T. K.; Min, B. Y. *J. Macromol. Sci., Chem.* **1984**, *A21*, 1181.
- (20) Bank, M.; Leffingwell, J.; Thies, C. J. *Polym. Sci., Polym. Phys. Ed.* **1972**, *10*, 1097.
- (21) Qin, C.; Cheng, C.; Pires, A. T. N.; Belfiore, L. A. *Polym. Mater. Sci. Eng.* **1989**, *61*, 945.
- (22) Patterson, D.; Robard, A. *Macromolecules* **1978**, *11*, 690.
- (23) Allcock, H. R. *Phosphorus-Nitrogen Compounds*; Academic Press: New York, 1972 and references therein.
- (24) Serman, C. J.; Xu, Y.; Painter, P. C.; Coleman, M. M. *Polymer* **1991**, *32*, 517.
- (25) Moskala, E. J.; Varnell, D. F.; Coleman, M. M. *Polymer* **1985**, *26*, 228.
- (26) Fettes, E. M. *Chemical Reactions of Polymers*; Wiley Interscience: New York, 1964; p 28.
- (27) Allcock, H. R. *Acc. Chem. Res.* **1979**, *12*, 351.